

# Jet Interaction in a Still Ambient Fluid

H. J. Wang<sup>1</sup> and M. J. Davidson<sup>2</sup>

**Abstract:** Interaction between a jet and its neighbors in a still ambient fluid is dealt with. A model for the merging of an infinite line of equally spaced identical jets in a still ambient fluid is developed. The velocity and tracer distributions in the model are determined based on the summation of momentum fluxes and tracer fluxes, respectively. Laser-induced fluorescence experiments are conducted for four different port spacings. Analysis of these and past experimental results show that individual jets spread asymmetrically during the merging process. The current model satisfactorily predicts the spreading rate changes in the free entrainment plane and the jet merging plane, as well as the tracer distributions during the merging process. Flapping motions were observed during jet merging, but these motions were not sufficiently persistent to significantly change the concentration fluctuations profiles.

**DOI:** 10.1061/(ASCE)0733-9429(2003)129:5(349)

**CE Database subject headings:** Hydraulic jets; Fluid; Interactions; Models.

## Introduction

Although, in general, wastewater disposal systems are designed to prevent the interaction of neighboring discharges, where the flows being disposed of are large it may not be possible to provide sufficient spacing between the discharges. Under these circumstances, discharges may interact and merge to form a combined flow, with a significant impact on the dilution efficiency of the system. This potential problem has, in part, provided the motivation for studying two-dimensional discharges, for example, Kotsovinos (1977) and Kotsovinos and List (1977), finite line discharges (Roberts 1979), and closely spaced radially discharged flows (Roberts and Snyder 1993).

Less common are studies that focus on the interaction and merging of closely spaced discharges. Knystautas (1964) studied the merging of a long line of identical jets in a still ambient fluid. In this situation, fluids released from the central ports are not influenced by edge effects and have two limits to their behavior. Initially where there is no interaction between neighboring discharges, the flow develops as a single axisymmetric jet. As the jets mix with the ambient fluid they grow and begin interacting with each other. Eventually they merge fully and reach the other limit, where their behavior resembles that of a two-dimensional jet.

Kynstautas conducted experiments where he measured velocity profiles in a line of merging jets in a still ambient fluid and two port spacings were considered. A merging still jet model was developed, based on an axisymmetric jet model that utilizes Reichardt's hypothesis. The merging of a line of jets was modeled by adding the momentum from each of the merging jets at a given

location. The overall momentum of the discharges was unchanged with downstream distance. With an appropriate definition of the spread function, the model correctly predicted the bulk behavior of the merging jets. Hodgson et al. (1999) extended Knystautas' model to provide predictions of tracer dilution. The spreading rate and the ratio of the concentration to the velocity length scales are assumed not to change during the merging process. A vacuum tube system was employed to obtain mean concentration profiles for a single port spacing and this data compares favorably with model predictions.

Davidson (1989) considered the problem of the merging of a line of jets in a coflowing ambient fluid. An additive assumption was employed to define the velocity distribution and concentration distribution of a merging jet. This approach is consistent with the summation of excess momentum and the summation of tracer flux in the weak jet (strongly advected) region. However, when applied to the merging jet problem in the strong jet (weakly advected) region or in a still ambient fluid, this approach is inconsistent with the summation of jet excess momentum flux and the summation of jet tracer flux. This inconsistency is only apparent during merging and the model correctly predicts the flow behavior in the axisymmetric and two-dimensional limits. Papps and Wood (1997) provided experimental evidence to support this for buoyant discharges in a still ambient fluid, although some modification of the model was required to account for flapping of the merged flow.

It is interesting to note, however, that none of the above models have considered the possible change in spreading rate that occurs when jets merge and move from the axisymmetric to the two-dimensional limit. These differences in spreading rates are evident in previous experimental studies of axisymmetric and two-dimensional jets (Fischer et al. 1979). The studies suggest a 10 to 20% increase in the spreading rate during the merging process. Other changes are also evident in existing experimental data sets and additional insight can be obtained through further experimental investigations into the behavior of merging jets.

In this paper, we return to the relatively simple problem of a line of merging jets in a still ambient fluid. We begin by developing a model based on the summation of jet momentum and tracer fluxes (similar to those developed previously by Knystautas and Hodgson et al.). However, the model presented here includes

<sup>1</sup>ESSC, Univ. of Reading, Harry Pitt Building, 3 Earley Gate, Reading RG6 6AL, U.K.

<sup>2</sup>Dept. of Civil Engineering, Canterbury Univ., Private Bag 4800, Christchurch, New Zealand. E-mail: mark.davidson@canterbury.ac.nz

Note. Discussion open until October 1, 2003. Separate discussions must be submitted for individual papers. To extend the closing date by one month, a written request must be filed with the ASCE Managing Editor. The manuscript for this paper was submitted for review and possible publication on May 14, 2001; approved on December 16, 2002. This paper is part of the *Journal of Hydraulic Engineering*, Vol. 129, No. 5, May 1, 2003. ©ASCE, ISSN 0733-9429/2003/5-349-357/\$18.00.

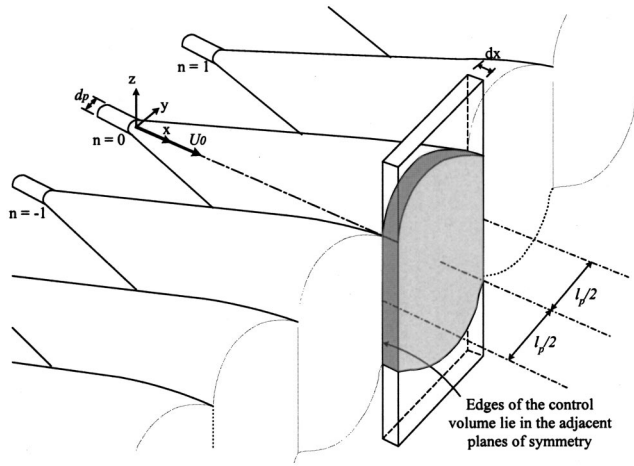


**Fig. 1.** Schematic diagram of a line of merging jets and control volume that is used to analyze their behavior. This figure also shows system employed for numbering ports.

the previously observed changes in the spreading rates and concentration to velocity length scale ratio between the axisymmetric and two-dimensional flow limits. The problem is then investigated experimentally using the laser-induced fluorescence technique. Detailed mean and fluctuating concentration fields are obtained for four port spacings. The results of this experimental investigation are compared with the predictions from the present model and those from Davidson (1989), Knystautas (1964), and Hodgson et al. (1999).

### Modeling Merging Jets in a Still Environment

The merging scenario considered here occurs when a line of identical axisymmetric jets are released from ports that are equally spaced at a distance  $l_p$ . The port diameter is  $d_p$ , and the jets are discharged at an initial velocity  $U_0$ , into an essentially infinite receiving fluid of the same density. In the analysis, a control volume centered on one of the central ports is employed and it extends a distance  $l_p$  in the  $y$  direction. The discharge configuration and the control volume are shown in Fig. 1.

The symmetry of the problem indicates that there will be no net momentum exchange between adjacent jets, so applying conservation of momentum to the control volume gives

$$I_M U^2 b l_p = M_{0,3D} \quad (1)$$

where  $M_{0,3D} = \pi U_0^2 d_p^2 / 4$ ;  $U$  = centerline mean velocity of the jet; and  $b$  = spread of the jet in the free entrainment ( $x$ - $z$ ) plane. This spread is defined as the radius at which the local mean velocity  $u = e^{-1} U$ , and the shape factor is defined by

$$I_M = \int_{-\infty}^{\infty} \int_{l_p/2}^{l_p/2} \left[ \frac{u}{U} \right]^2 \frac{dy}{l_p} \frac{dz}{b} \quad (2)$$

Introducing a tracer of concentration ( $C_0$ ) at the source and conserving the concentration of this tracer as it passes through the cylindrical control volume yields

$$I_{QC} U C b l_p = C_0 Q_{0,3D} \quad (3)$$

where  $Q_{0,3D} = \text{initial discharge } (\pi U_0 d_p^2 / 4)$ ; and  $C$  = centerline tracer concentration; and the shape constant is given by

$$I_{QC} = \int_{-\infty}^{\infty} \int_{l_p/2}^{l_p/2} \left[ \frac{cu}{CU} \right] \frac{dy}{l_p} \frac{dz}{b} \quad (4)$$

Note that  $c$  is the local mean concentration. It is commonly accepted that both the mean velocity and concentration distributions of jets (in the free entrainment plane of the problem considered here) can be approximated by normal distributions. They can therefore be modeled using the following functions:

$$\frac{u}{U} = e^{-(r/b)^2} \quad (5)$$

$$\frac{c}{C} = e^{-(r/\lambda b)^2} \quad (6)$$

where  $r$  = radial coordinate. The spread assumption, which assumes a linear growth with distance from the source, can then be employed to close the system of equations. However, although the velocity and tracer distributions in the  $x$ - $z$  plane remain Gaussian and self similar throughout the merging process, in the  $x$ - $y$  plane this is no longer true. The velocity and concentration distributions are initially Gaussian, but after merging they are uniform. To obtain a solution, the velocity and tracer distributions must be defined during merging.

It is appropriate to add the conserved quantities and hence we sum the merging jet momentum to obtain the velocity distribution and the tracer flux to yield the concentration distribution, during the merging process. The velocity distribution is obtained by initially considering the momentum flux ( $dM$ ) passing through an elemental area  $dA$ , before merging takes place (the axisymmetric limit). This can be expressed as

$$dM = u^2 dA = u_{\text{axi}}^2 dA \quad (7)$$

where  $u_{\text{axi}}$  = local axisymmetric jet velocity. However, as merging takes place, the momentum flux through the same element of area becomes

$$dM = u^2 dA = \left( \sum_{n=-\infty}^{n=\infty} u_{\text{axi}}^2(n) \right) dA \quad (8)$$

where  $n$  = port number.

Similarly, the tracer flux passing through the same elemental area ( $dQC$ ) before merging begins is

$$dQC = uc dA = u_{\text{axi}} c_{\text{axi}} dA \quad (9)$$

where  $c_{\text{axi}}$  = local axisymmetric jet tracer concentration. During the merging process the tracer flux becomes

$$dQC = uc dA = \left( \sum_{n=-\infty}^{n=\infty} u_{\text{axi}} c_{\text{axi}}(n) \right) dA \quad (10)$$

Eqs. (8) and (10) provide the basis for developing general expressions for the velocity and tracer distributions during merging. Making use of Eqs. (5) and (6), expressions for the axisymmetric velocity and concentration profiles for each of the jets can be written as

$$\frac{u_{\text{axi}}}{U} = e^{-(z/b)^2} e^{-((y+n\ell_p)/b)^2} \quad (11)$$

$$\frac{c_{\text{axi}}}{C} = e^{-(z/\lambda b)^2} e^{-((y+\ell_p)/\lambda b)^2} \quad (12)$$

These expressions can be substituted into Eqs. (8) and (10) and

the appropriate expressions for the centerline values of the combined flows can then be determined. The velocity and tracer distributions are then written as

$$\frac{u}{U} = \left[ \frac{\exp\left\{-2\left[\frac{z}{b}\right]^2\right\} \sum_{n=-\infty}^{\infty} \exp\left\{-2\left[\frac{y+nl_p}{b}\right]^2\right\}}{\sum_{n=-\infty}^{\infty} \exp\left\{-2\left[\frac{nl_p}{b}\right]^2\right\}} \right]^{1/2} \quad (13)$$

$$\frac{uc}{UC} = \frac{\exp\left\{-\left[\frac{\sqrt{1+\lambda^2}z}{\lambda b}\right]^2\right\} \sum_{n=-\infty}^{\infty} \exp\left\{-\left[\frac{y+nl_p}{b}\right]^2\left[\frac{1+\lambda^2}{\lambda^2}\right]\right\}}{\sum_{n=-\infty}^{\infty} \exp\left\{-\left[\frac{nl_p}{b}\right]^2\left[\frac{1+\lambda^2}{\lambda^2}\right]\right\}} \quad (14)$$

The values of shape factors  $I_M$  and  $I_{QC}$  are then determined by substituting Eqs. (13) and (14) into Eqs. (2) and (4). Simplification of the resulting integrals requires the integration of summations of the following form:

$$\Sigma_1 = \sum_{n=-\infty}^{\infty} \exp\left\{-2\left[\frac{\Psi+n}{\Omega}\right]^2\right\} \quad (15)$$

where  $\Psi = y/\ell_p$  and  $\Omega = b/\ell_p$  or  $b\lambda/\ell_p[1+\lambda^2]^{1/2}$ .

With some manipulation, this summation can be written in the alternative form of a  $\theta_3$  function as described by Fenton and Gardiner-Garden (1982)

$$\begin{aligned} \Sigma_1 &= \exp\left\{-2\left[\frac{\Psi}{\Omega}\right]^2\right\} \left[ 1 + 2 \sum_{n=1}^{\infty} \exp\left\{-2\left[\frac{n}{\Omega}\right]^2\right\} \cosh\left\{\frac{4\Psi n}{\Omega^2}\right\} \right] \\ &= \sqrt{\frac{\pi}{2}} \Omega \theta_3 \left\{ \pi \Psi, \exp\left\{-\frac{[\pi\Omega]^2}{2}\right\} \right\} \end{aligned} \quad (16)$$

Making use of the conventional form of the  $\theta_3$  function, the summation then becomes

$$\begin{aligned} &\sqrt{\frac{\pi}{2}} \Omega \theta_3 \left\{ \pi \Psi \exp\left\{-\frac{[\pi\Omega]^2}{2}\right\} \right\} \\ &= \sqrt{\frac{\pi}{2}} \Omega \left[ 1 + 2 \sum_{n=1}^{\infty} \exp\left\{-\frac{[\pi\Omega n]^2}{2}\right\} \cosh\{2n\pi\Psi\} \right] \\ &= \Sigma_1 \end{aligned} \quad (17)$$

Manipulating the summations in this way simplifies the shape factor integrations, which yield the following relationships:

$$\frac{I_M}{1.11} = \frac{\sqrt{\frac{\pi}{2}}}{1 + 2 \sum_{n=1}^{\infty} \exp\left\{-\left[\frac{n\pi b}{\sqrt{2}l_p}\right]^2\right\}} \quad (18)$$

$$\frac{I_{QC}}{1.08} = \frac{\lambda \sqrt{\pi}}{[1 + \lambda^2]^{1/2} \left[ 1 + 2 \sum_{n=1}^{\infty} \exp\left\{-\left[\frac{n\pi b}{l_p}\right]^2 \left[\frac{\lambda^2}{1 + \lambda^2}\right]\right\} \right]} \quad (19)$$

The constants 1.11 and 1.08 have been added to take account of the turbulent flux terms. These values are based on the axisymmetric limit.

During merging, the values of the spread constant  $k$  and the length-scale ratio  $\lambda$  must be transformed from their axisymmetric values to their two-dimensional values. A linear approximation is

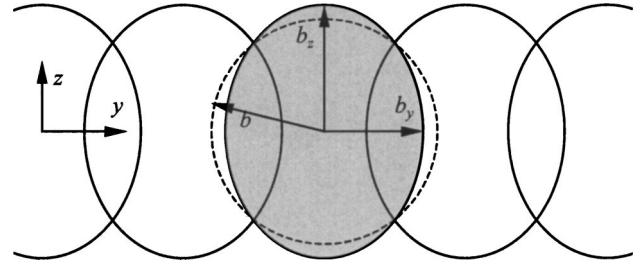


Fig. 2. Schematic diagram of jet deformation during merging process

employed to make this transformation, because the details of these changes are not known.

The present experiments indicate that there are also differences between the values of the spread parameter  $k$  and the length-scale ratio  $\lambda$  in the  $x$ - $y$  and  $x$ - $z$  planes during the merging process, as is indicated in the schematic diagram in Fig. 2. To allow for this in the model, the spreading rate and the concentration to velocity spread ratio are defined separately for the two directions.

The velocity distributions and tracer concentration distributions in the  $x$ - $y$  and  $x$ - $z$  planes are therefore determined based on the spreading rates in specific directions. To simplify the model, the cross-sectional area of an individual jet during merging has been assumed to have an elliptical shape, so that the merging of axisymmetric jets is simulated as the merging of elliptical jets. The long axis of each ellipse is  $b_z$ , the short axis is  $b_y$ , and the area is equivalent to a circular area with a radius of  $b$ , as shown in Fig. 2. The cross-sectional area of velocity field is then

$$A = \pi b_y b_z = \pi b^2 \quad (20)$$

and the cross-sectional area of concentration field is given by

$$A_c = \pi b_{c,y} b_{c,z} = \pi b_c^2 \quad (21)$$

Eqs. (18) and (19) show that the shape parameters are no longer constant with respect to downstream distance, but are instead a function of the ratio of the jet spread to port spacing ( $b_y/l_p$ ). Fig. 3 shows how these shape parameters vary as this ratio increases. Note that the spread in the  $x$ - $y$  plane ( $b_y$ ) is the relevant jet scale for determining the extent of jet merging.

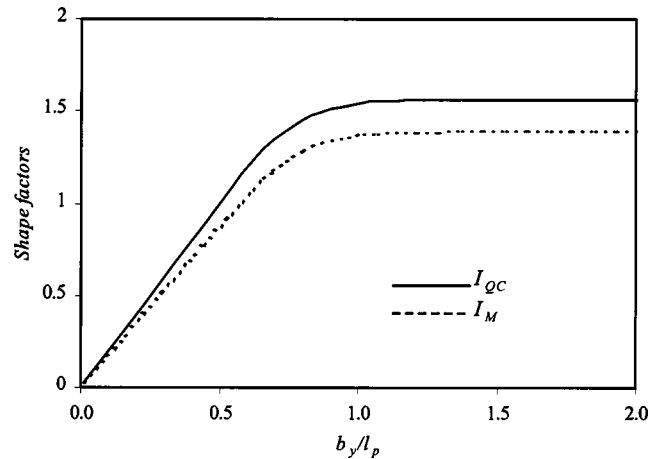


Fig. 3. Variation of shape parameters  $I_M$  and  $I_{QC}$  with spread-to-port ratio ( $b_y/l_p$ )

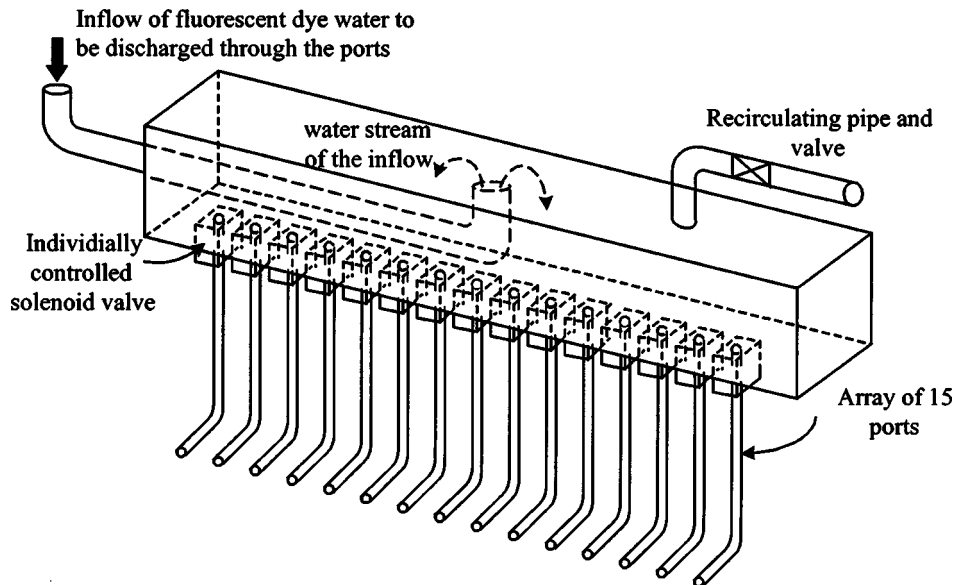


Fig. 4. Schematic diagram of manifold system used to distribute flow to 15 discharge pipes

In the axisymmetric limit, the shape parameters become  $I_M = I_{M,3D} b_y / l_p$  and  $I_{QC} = I_{QC,3D} b_y / l_p$ . The conservation of momentum flux and conservation of tracer flux equations are then reduced to their axisymmetric form. A noticeable change (1%) in the gradient of the shape parameters occurs after  $x/l_p$  reaches 4.5 ( $b_y/l_p$  is about 0.5). This indicates the location where the interference of individual jets becomes strong enough to affect the bulk properties of the central jet. The flow reaches its two-dimensional limit when  $x/l_p \approx 12$ . In the two-dimensional limit, the shape parameters take on their two-dimensional values, that is,  $I_M = I_{M,2D}$  and  $I_{QC} = I_{QC,2D}$ . This then gives the two-dimensional form of the conservation of momentum and tracer flux equations. The merging region is therefore defined by  $4.5 < x/l_p < 12$  and this provides the basis for linear transformations of the spread ( $k$ ) and the length-scale ratio ( $\lambda$ ) values.

Eqs. (18) and (19) can also be used to estimate the minimum number of discharges required, before the central flows behave as if the line of discharges were infinite. This is done by reducing the number of discharges ( $2n + 1$ ) over which the summation occurs, until a 1% variation is detected in the values of the shape parameters. Adopting this approach, the minimum number of discharges required to satisfy this condition is 13. It is worth noting that although one can simply reduce  $n$  in an attempt to model small groups of merging jets, other physical processes (not dealt with in the model) may then become important. For example, if just three jets are released, asymmetries in the demand for entrained fluid may create significant pressure gradients that draw the flows together.

## Experimental Design

An experimental investigation into the merging of jets in a still ambient fluid was carried out in the Water Resources Research Laboratory at the Hong Kong University of Science and Technology. This laboratory houses a towing tank that is 15 m in length, 2 m wide, and 1.6 m deep. The towing tank was filled to a depth of 1.2 m. Fifteen equally spaced pipes were mounted on a computer-controlled carriage, so that they discharged horizontally into the tank at a depth of 600 mm. Two sets of these pipes

(internal diameters were 4.64 and 1.77 mm) were employed in the experiments. The 15 pipes were connected to a manifold located above the water surface and this was used to distribute the total source flow evenly to the pipes. The variation in the discharge from the pipes was kept to within 5% of the average value. A schematic diagram of the manifold system is shown in Fig. 4. The source and ambient fluids were both fresh water and the densities of these fluids were accurately monitored using a precision density meter (PAAR DMA58).

A laser-induced fluorescence (LIF) system was employed to record the behavior of the merging jets. The light source for the system was a 6 W Argon Laser that was operated in a single mode at a wavelength of 514 nm. The laser light power was set at 2.0 W for these experiments. The laser beam passed onto a rotating mirror that scanned the beam across a parabolic mirror. This combination of mirrors produced a parallel-planar light sheet. The light sheet was approximately 500 mm wide and 5 mm thick. During the experiments, the towing tank was completely isolated from the remainder of the laboratory using black laser safety curtains and this effectively eliminated all extraneous light sources.

The behavior of the merging jets, in the light sheet, was observed by adding a fluorescent dye tracer to the source fluid. The dye tracer was Rhodamine 590. This dye fluoresces when illuminated with light of wavelength 514 nm and emits light at a wavelength of 590 nm. The observation system consisted of a low-light security video camera (Panasonic WV-BP510/G) and a video recorder (Panasonic AG-6730). The Panasonic camera was operated such that its automatic light compensation features were inactivated. The camera was fitted with a filter that eliminated light at a wavelength of 514 nm, thus the only light recorded by the observation system was that generated by the fluorescing dye. A schematic diagram of the experimental system is shown in Fig. 5. For some of the experiments, the laser sheet was located in a horizontal plane and the video camera was moved to give a plan view of merging jet behavior. The video images were later digitized using a Data Translation (DT2867) image capture board and processed on a PC.

The images of the merging jets were converted to quantitative concentration data through the image processing system. The pro-

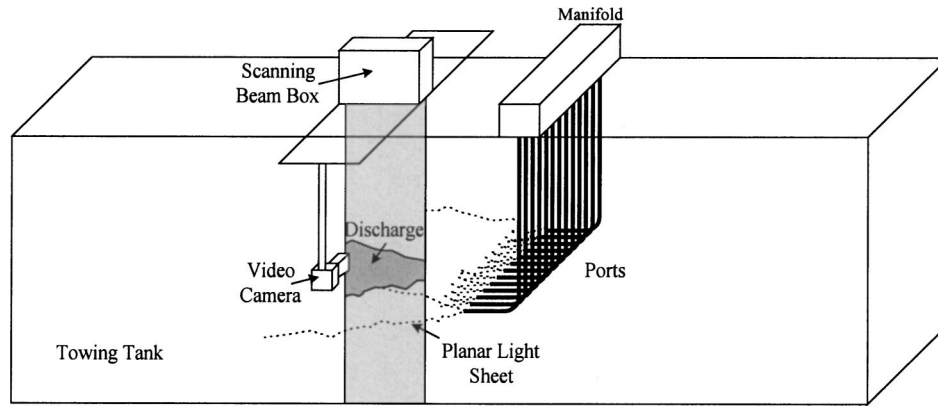


Fig. 5. Schematic diagram of LIF system used to record behavior of merging jets

cessing of the digitized images involved removing background light, correcting for variations in the source light intensity and calibrating the image so that the intensity of light at each pixel was directly and consistently related to tracer concentration. A more detailed explanation of the processes involved is contained in Wang (2000). Digitized images of a 50 mm × 50 mm grid were also analyzed to provide spatial calibrations for the images. Typically, for each experiment a set of 200 to 300 images were digitized at a rate of 1 Hz. An average of these images provided details about the mean behavior of the merging jets. The complete set of images were also analyzed to provide information on fluctuation statistics such as the root-mean square and intermittency of the concentration fluctuations.

## Model Predictions and Experimental Results

### Mean Properties

The merging jet model assumes that the tracer and velocity profiles are Gaussian and self similar throughout the merging process in the  $x$ - $z$  plane, but that these profiles transform from a Gaussian to a uniform distribution in the  $x$ - $y$  plane. Tracer profiles taken from the  $x$ - $z$  plane are shown in Fig. 6 and those from the  $x$ - $y$

plane are shown in Fig. 7. The Gaussian and self-similar nature of the tracer profiles throughout the merging process in the  $x$ - $z$  plane is evident in Fig. 6. In contrast, the profiles in Fig. 7 are no longer self similar, changing from being Gaussian as merging commences to become uniform as the merging process is complete.

The mean centerline concentration and concentration spread in the  $z$  direction can be obtained by fitting Gaussian distributions to the tracer profiles in the  $x$ - $z$  plane. While the concentration spread in the  $y$  direction can be obtained by comparing the concentration distribution obtained from Eqs. (13) and (14) with tracer profiles in the  $x$ - $y$  plane. It is worth noting that as merging nears completion the data obtained for spread in the  $y$  direction becomes less reliable. This is because the profiles become increasingly uniform. However, the magnitude of spread in this direction is also becoming less important and is no longer significant once merging is complete. In the context of concentration spread merging appears to have taken place as  $x/l_p$  approaches 11. The concentration-spread variations in both  $x$ - $y$  and  $x$ - $z$  directions along the jet trajectory are shown in Fig. 8, where they are compared with model predictions.

Fig. 8 is plotted with  $x$  and  $b_c$  normalized by the port spacing  $l_p$  so that all the experimental data obtained in the same observation plane, with different port spacing ratios ( $l_p/d_p$ ), collapse to a single line. It is clear from Fig. 8 that the concentration spread-

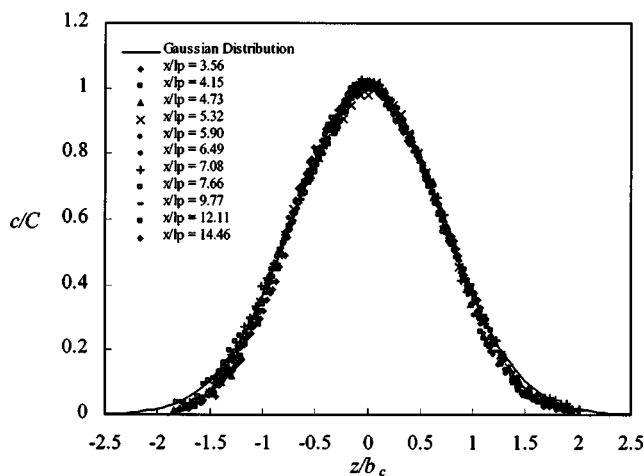


Fig. 6. Measured tracer distributions during merging of jets in still ambient fluid in  $x$ - $z$  plane, with port Reynolds number 2660 and port spacing  $34d_p$

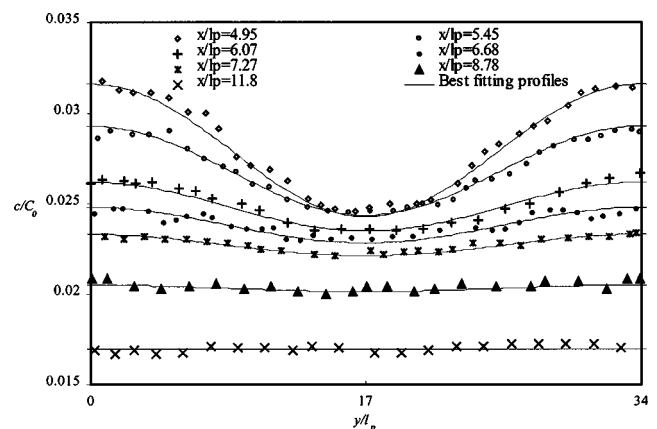
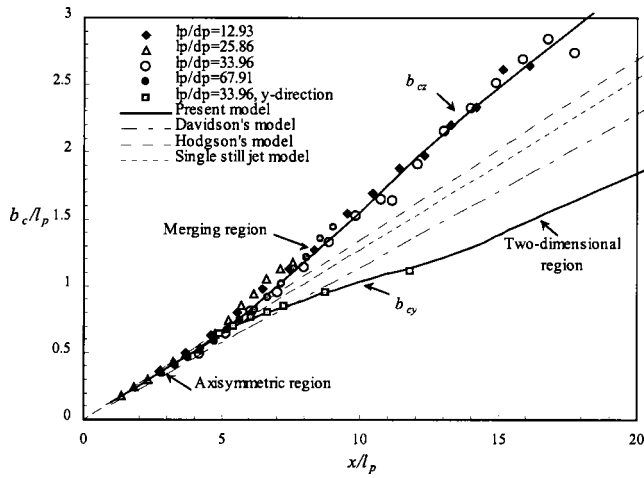


Fig. 7. Measured mean concentration profiles during merging of jets in a still ambient fluid in  $x$ - $y$  plane, with port Reynolds number 2660 and port spacing  $34d_p$ . Eqs. (13) and (14), with  $\lambda_y = 1.15$ , have been used to plot curves which are shown for comparison.



**Fig. 8.** Spread of merging jet tracer profiles in  $x$ - $y$  and  $x$ - $z$  planes as function of downstream distance. Initial Reynolds number for data was 2,660 to 5,500.

ing rate in the  $x$ - $z$  plane increases during the jet merging process, and the increase is about 30% from the axisymmetric to the two-dimensional limit. In contrast, the concentration spread rate in the  $x$ - $y$  plane decreases by a similar amount from the axisymmetric to the two-dimensional limit. The value of  $k\lambda$  in the  $z$  direction varies from 0.127 to 0.165 and in the  $y$  direction the data suggests the variation is from 0.127 to approximately 0.092 during jet merging. These results indicate the growth of individual jets is no longer axisymmetric once the interference from neighboring jets is sufficiently strong.

The changes in growth rates during jet merging are not only observed in the present experiments, but are also evident in the velocity data obtained by Knystautas (1964). This can be seen in Figs. 9 and 12, where there is some inconsistency between models that assume a constant growth rate during jet merging and his experimental data. The velocity profiles measured in the  $x$ - $y$  plane, from which the spread data shown in Fig. 9 were obtained, indicate that merging nears completion as  $x/l_p$  approaches 13.

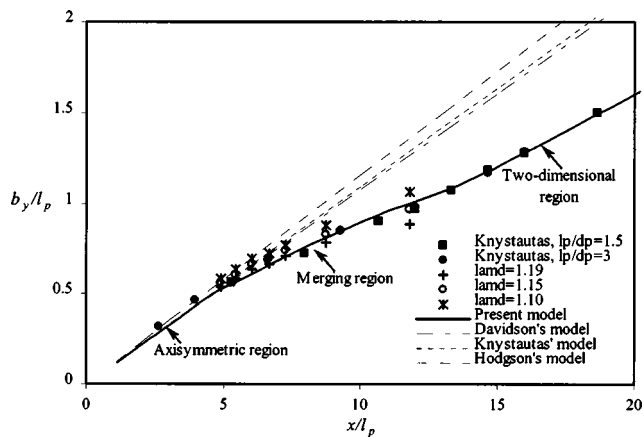


**Fig. 9.** Comparison of model predictions for velocity spread in  $x$ - $y$  plane. Data from Knystautas (1964) and current study are shown for comparison. Value of spread constant  $k$  used in present model varies from 0.107 to 0.08 in  $x$ - $y$  plane during jet merging.

The tracer profiles therefore become uniform in advance of the velocity profiles and this is consistent with differences in their respective rates of spread.

The increased growth rate in the  $x$ - $z$  plane indicates that the interaction between jets during the merging process increases the rate of jet entrainment in the free entrainment ( $x$ - $z$ ) plane. This observation is also consistent with previous experimental results that indicate that the spreading rate of a two-dimensional jet is significantly larger than that of an axisymmetric jet. In the  $x$ - $y$  plane, it appears that the jet entrainment is suppressed by the presence of the neighboring jets. This results in a reduction in spread in the  $y$  direction. The merging process reduces the mean shear in the  $x$ - $y$  plane and limits the scale of the large eddies in this plane. These eddies are largely responsible for initiating the entrainment and energy dissipation processes. It is conceivable therefore, that more energy will be dissipated by the large eddy motions in the  $x$ - $z$  plane, which in turn enhances entrainment and spread in that plane.

As velocity (Knystautas 1964) and concentration profiles (shown in Fig. 7) in the  $x$ - $y$  plane are both available, it is therefore possible to obtain an estimate of the values of  $b_y$  and  $b_{cy}$  at each location during jet merging. This can be achieved by fitting the velocity and concentration distributions obtained from Eqs. (13) and (14) to the experimental data, as was done for Fig. 7. The variations of velocity spread parameter ( $k$ ) and the ratio of the tracer to velocity spread ( $\lambda$ ) can therefore be determined in the  $x$ - $y$  plane. Fig. 9 shows the velocity spread  $b_y$  from Knystautas' study as well as data obtained from the current study by dividing the concentration spread with different  $\lambda$  values.

In this figure, it is evident that Knystautas' data is in good agreement with the model predictions when the value of spread constant  $k$  varies from 0.107 to 0.08 in the  $x$ - $y$  plane during jet merging. Typically, in the axisymmetric region of these flows  $\lambda$  is assumed to be 1.19 and velocity spread values determined from the present study (based on this value of  $\lambda$ ) are consistent with Knystautas experimental data. However, a value of  $\lambda = 1.15$  is required to maintain this consistency as merging takes place. The data therefore suggests the following values for the spread related constants:

$$k_{y,3D} = k_{z,3D} = 0.107 \quad \lambda_{y,3D} = \lambda_{z,3D} = 1.19$$

$$k_{z,2D} = 0.118 \quad \lambda_{z,2D} = 1.40$$

$$k_{y,2D} = 0.08 \quad \lambda_{y,2D} = 1.15$$

It is worth noting that once a two-dimensional flow forms, the values of spread constants  $k$  and  $\lambda$  in the  $y$  direction are no longer significant, because the flow behavior is only affected by the parameters in the  $x$ - $z$  plane. Therefore, the values of  $k_{y,2D}$  and  $\lambda_{y,2D}$  are only employed to create the correct behavior in the merging region. It should also be noted that the uneven growth in the  $y$  and  $z$  directions starts when  $x/l_p$  is approximately 4.5 ( $b_y/l_p \approx 0.5$ ).

The significance of the difference the above modifications make to the model predictions can be seen in Fig. 10. Here, a concentration profile measured in the  $x$ - $y$  plane at a distance of 247 port diameters ( $x/l_p = 7.27$ ) from the flow sources is shown. Predictions from the present model and models developed by Davidson (1989) and Hodgson et al. (1999) are shown for comparison. Both models assume symmetrical spreading during the merging process and in doing so they overestimate the interaction of the jets in the  $x$ - $y$  plane and hence the predicted concentration profiles show a greater degree of merging than is indicated by the data. The additive assumption employed in Davidson's model tends to augment this problem because it overpredicts velocities

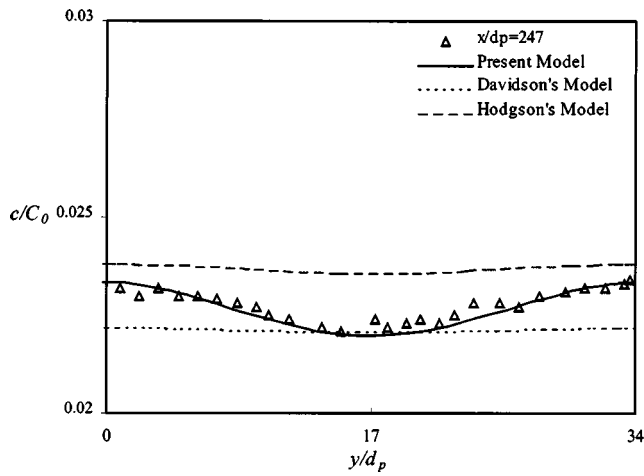


**Fig. 10.** Model predictions compared with measured tracer data at  $x/d_p = 247$  during merging of jets in a still ambient fluid. Profile was recorded in  $x$ - $y$  plane. Port Reynolds number was 2,660 and port spacing was  $34d_p$ .

near the planes of symmetry between the jets and underpredicts velocities near the flow centerline. Fig. 10 also shows how the differences in the choice of parameter values for the two-dimensional region can significantly affect the predicted values. For example, Davidson's model makes use of a relatively large value (1.19) for the turbulent fluctuation term in the shape factor  $I_{QC}$  and the relatively low value (1.067) for the spread ratio  $\lambda$ . Its predictions of tracer concentration are therefore generally lower than the other models.

Centerline dilution data obtained from present experiments are plotted in Fig. 11, where the data obtained by Hodgson et al. (1999) and model predictions are also shown for comparison. In Fig. 12, the velocities calculated from the dilution and spread data are shown together with Knystautas' experimental data and model predictions. The model described in this paper is able to accurately predict the dilution and velocity of the merging flows before, after, and during the jet merging process. The predictions are generally better than those of previous developed models and this is largely because the experiments' results have provided the basis for more accurately defining the empirical parameters in the

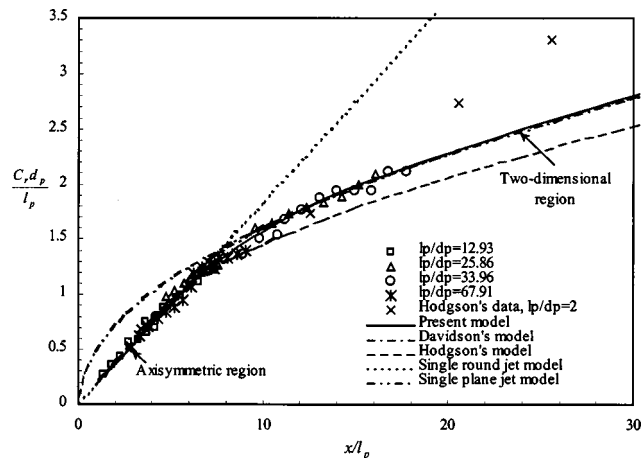


**Fig. 11.** Dilution of merging jets as function of downstream distance. Initial Reynolds number for this data ranges from 2,660 to 5,500.

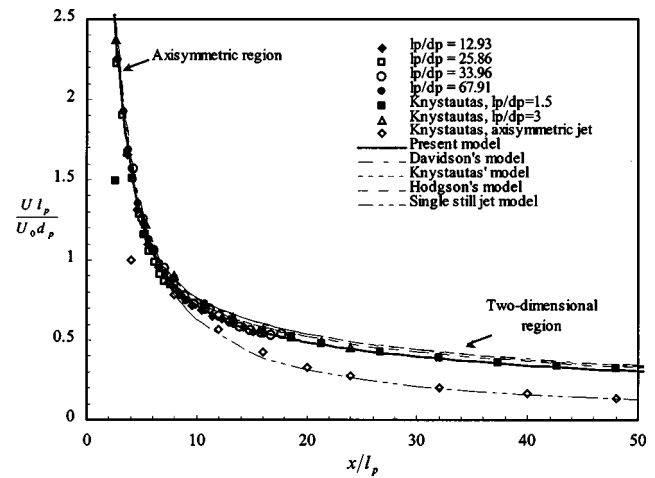


**Fig. 12.** Calculated velocity of merging jets as function of downstream distance. Initial Reynolds number for this data was 2,660 to 5,500. Knystautas' experimental data are also shown for comparison.

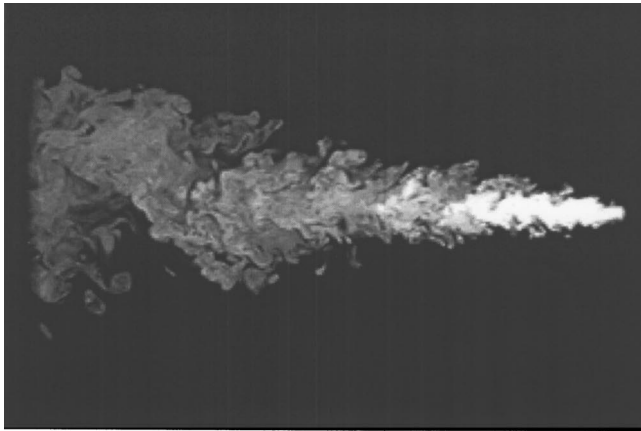
present model. Of particular importance is the incorporation of changes that occur to the shape of the individual jets as merging take places.

It is worth noting that the Hodgson et al. dilution data (Fig. 11) were obtained from experiments with just three identical merging jets. It is evident that shortly after the three jets merge, the central jet behavior is similar to that of a jet in a much larger line of identical jets (as in the present study). However, as the merging develops further, the dilution rate of the small group of merging jets changes to become more like that of an axisymmetric jet. This indicates the importance of the jet's immediate neighbors during the initial phase of merging, but that the presence of the remaining jets in the line becomes increasingly important as the merging process continues.

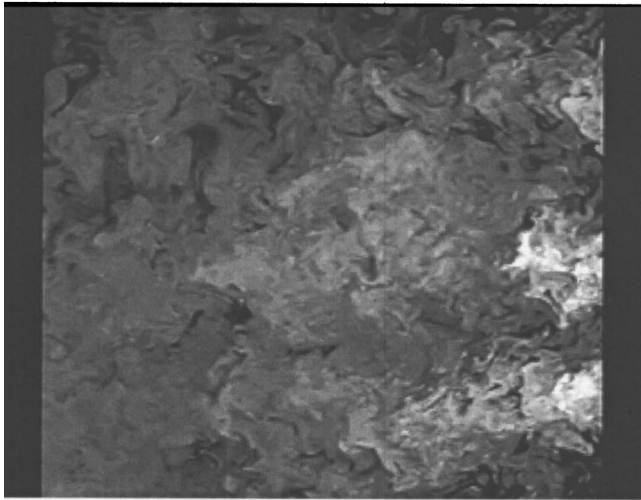
### Mixing Process and Concentration Fluctuations During Jet Merging

Figs. 13(a and b) show the instantaneous images of merging jets. The image shown in Fig. 13(a) was taken in the  $x$ - $z$  plane and an image taken in the  $x$ - $y$  plane is shown in Fig. 13(b). Changes to the structure of the flow are evident in the  $x$ - $z$  plane. Large-scale flapping structures, typical of two-dimensional jets (Goldschmidt and Bradshaw 1973; Kotsovinos 1977; Goldschmidt et al. 1983; Dracos et al. 1992; Papps and Wood 1997), can be seen forming in the region where merging takes place and these structures enhance the growth of the jet. In contrast, the image of the  $x$ - $y$  plane [Fig. 13(b)] shows a more uniform range of eddy scales and relatively well-mixed tracer solution in the region where merging is taking place. In this plane, as merging takes place the jets are entraining each other and the concentration gradients are reduced. In addition, the mean shear is reduced and the vortices in the merging jets have a tendency to cancel each other out. The overall effect being a reduction in the efficiency of the mixing process when compared to an axisymmetric flow. Ambient fluid can only reach the central regions of the flow through the action of the large eddies in the  $x$ - $z$  plane and hence the jet dilutes relatively slowly.

Fluctuation statistics for the merging flows were obtained by comparing a large number (in excess of 200) of instantaneous images with the average of those images. It is important to bear in mind that the images have been captured at a frequency of 1 Hz



(a)



(b)

**Fig. 13.** Instantaneous images of merging jets taken in experiments for both  $x$ - $y$  plane and  $x$ - $z$  plane. (a) Instantaneous image of merging jets taken in  $x$ - $z$  plane. (b) Instantaneous image of merging jets taken in  $x$ - $y$  plane.

and hence contributions from higher-frequency fluctuations will not be resolved with this system. In addition, the spatial resolution of the images is approximately 0.7 mm in the  $x$  and  $z$  directions. Representative data for the root-mean square of the concentration fluctuations in a merging jet is shown in Fig. 14. The strength of fluctuations is consistent with that expected for an axisymmetric flow and the profiles are essentially self similar. It is interesting to note that the strength of the fluctuations does not increase significantly as merging takes place. This indicates that in the regions observed, the impact of the flapping motion of the flow was not persistent enough to significantly alter the fluctuation statistics of the flow. However, it is worth noting that comparisons between the data obtained by Papanicolaou (1984) for axisymmetric jets and of Kotsovinos (1977) for plane buoyant jets suggest that the relative strength of the fluctuations should increase as merging takes place. The difference may result from the fact that in the present study the flows have only been observed near the region where merging takes place. The flapping motion may become more persistent as the flow develops further down-

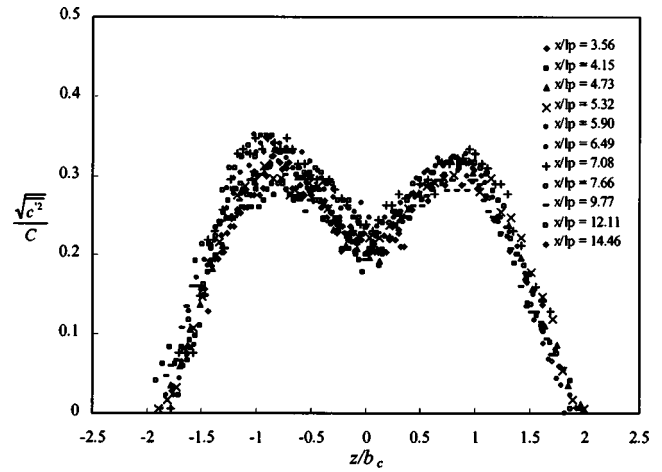


**Fig. 14.** Root-mean square of concentration signal at different locations in merging jet taken in  $x$ - $z$  plane, with port Reynolds number 2,660 and nondimensional port spacing 12.9

stream of this location and hence have a more significant impact on the fluctuation statistics.

Information on the intermittency of the concentration fluctuations can also be obtained from the images. The intermittency parameter represents the probability of exceeding a specified threshold value of concentration. Intermittency data for a merging jet is shown in Fig. 15. Here, the threshold value of the concentration was set at 0.0002 mg/l. The profiles remain essentially unchanged as merging takes place and again indicate that structural changes to the flow do not have a significant impact on the fluctuations statistics in the region where the flow was observed.

## Conclusions

A model for the merging of an infinite line of identical jets in a still ambient fluid has been developed. Following Knystautas (1964), the velocity distributions of the merging jets were obtained by summing the momentum fluxes of the merging flows. The model was then extended to provide dilution predictions and

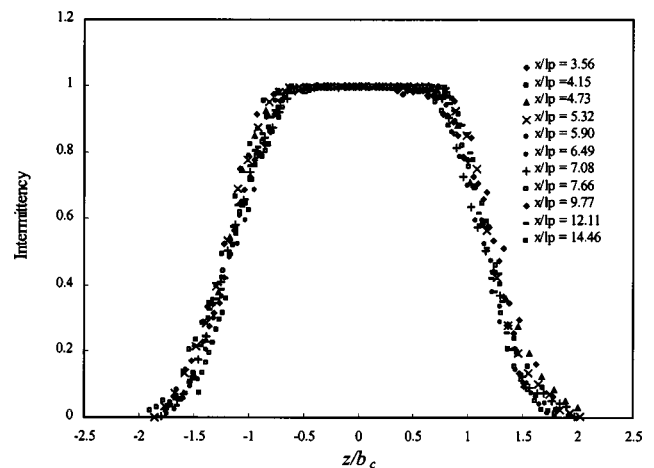


**Fig. 15.** Intermittency of concentration signal at different locations in merging jet measured in  $x$ - $z$  plane, with port Reynolds number 2,660 and nondimensional port spacing 12.9

the tracer distributions of the merging flow were determined by summing the tracer fluxes of the merging jets [similar to Hodgson's (1999) model]. Based on the dependence of the shape parameters on the number of jets present in the line, the model is applicable for modeling the merging of central jets when the number of jets exceeds 13.

The tracer distributions of merging jets were measured using laser-induced fluorescence and image processing systems. Data was obtained from merging discharges at four different port spacing ratios. The spread data obtained from the experiments shows that jet growth is asymmetric during jet merging. The jet growth is reduced in the merging direction, but enhanced in the direction where ambient fluid is freely entrained. This variation of the spreading rate in different directions is included in the present model, so that it is able to accurately predict the merging process and the dilution of the tracer as merging takes place.

Previously developed models that assume symmetric spreading during jet merging provide less accurate predictions of jet concentration and velocity distributions in the  $x$ - $y$  plane. In addition, those models that employ the summation of velocity and tracer distributions, to describe the merging flow, incorrectly distribute momentum and tracer in the jet cross section and because of this they have a tendency to underpredict centerline dilutions during jet merging.

The concentration fluctuation statistics of merging jets show that the flapping motion in the  $x$ - $z$  plane is not persistent enough to have any significant effect on the fluctuation statistic of the jets. The root-mean square of the concentration fluctuations relative to the local mean concentration and the intermittency of the concentration fluctuations do not change significantly as the flows merge. However, the flapping of the jet appears to be responsible for increasing the spreading rate of the merged flow in the  $x$ - $z$  plane.

## Acknowledgment

The writers acknowledge the financial support of the Research Grants Council of Hong Kong.

## References

- Davidson, M. J. (1989). "The behavior of single and multiple, horizontally discharged, buoyant flows in a nonturbulent coflowing ambient fluid." PhD thesis, Rep. 89-3, Dept. of Civil Engineering, Univ. of Canterbury, Christchurch, New Zealand.
- Dracos, T., Giger, M., and Jirka, G. H. (1992). "Plane turbulent jets in a bounded fluid layer." *J. Fluid Mech.*, 241, 587-614.
- Fenton, J. D., and Gardiner-Garden, R. S. (1982). "Rapidly-convergent methods for evaluating elliptic integrals and theta and elliptic functions." *J. Aust. Math. Soc. B, Appl. Math.*, 24, 47-58.
- Fischer, H. B., List, E. J., Koh, R. C. Y., Imberger, J., and Brooks, N. H. (1979). *Mixing in inland and coastal waters*, Academic, New York.
- Goldschmidt, V. W., and Bradshaw, P. (1973). "Flapping of a plane jet." *Phys. Fluids*, 16(3), 354-355.
- Goldschmidt, V. W., Moallemi, M. K., and Oler, J. W. (1983). "Structures and flow reversal in turbulent plane jet." *Phys. Fluids*, 26(2), 428-432.
- Hodgson, J. E., Moawad, A. K., and Rajaratnam, N. (1999). "Concentration field of multiple circular turbulent jets." *J. Hydraul. Res.*, 37(2), 249-256.
- Knystautas, R. (1964). "The turbulent jet from a series of holes in line." *Aeronaut. Q.*, XV, 1-28.
- Kotsovinos, N. E. (1977). "Turbulent buoyant jets. II: Turbulent structure." *J. Fluid Mech.*, 81, 45-62.
- Kotsovinos, N. E., and List, E. J. (1977). "Turbulent buoyant jets. I: Integral properties." *J. Fluid Mech.*, 81, 25-44.
- Papanicolaou, P. N. (1984). "Mass and momentum transport in a turbulent buoyant vertical axisymmetric jet." PhD thesis, W. M. Keck Laboratory of Hydraulic Resources, Division of Engineering and Applied Science, California Institute of Technology, Pasadena, Calif.
- Papps, D. A., and Wood, I. R. (1997). "The effect of an intermittent flapping motion on the properties of merging plumes." *J. Hydraul. Res.*, 35(4), 455-472.
- Roberts, P. J. W. (1979). "Line plume and ocean outfall dispersion." *J. Hydraul. Div., Am. Soc. Civ. Eng.*, 105(4), 313-331.
- Roberts, P. J. W., and Snyder, W. H. (1993). "Hydraulic model study for Boston outfall. I: Riser configuration." *J. Hydraul. Eng.*, 119(9), 970-987.
- Wang, H. J. (2000). "Jet interaction in a still or co-flowing environment." PhD thesis, Rep. 00-1, Dept. of Civil and Structural Engineering, The Hong Kong Univ. of Science and Technology, Hong Kong.